

A Unified View of the Role of Electrostatic Interactions in Modulating the Gating of Cys Loop Receptors*[§]

Received for publication, August 5, 2005, and in revised form, October 6, 2005 Published, JBC Papers in Press, October 10, 2005, DOI 10.1074/jbc.M508635200

Xinan Xiu, Ariele P. Hanek, Jinti Wang, Henry A. Lester, and Dennis A. Dougherty¹

From the Division of Chemistry and Chemical Engineering and Division of Biology, California Institute of Technology, Pasadena, California 91125

In the Cys loop superfamily of ligand-gated ion channels, a global conformational change, initiated by agonist binding, results in channel opening and the passage of ions across the cell membrane. The detailed mechanism of channel gating is a subject that has lent itself to both structural and electrophysiological studies. Here we defined a gating interface that incorporates elements from the ligand binding domain and transmembrane domain previously reported as integral to proper channel gating. An overall analysis of charged residues within the gating interface across the entire superfamily showed a conserved charging pattern, although no specific interacting ion pairs were conserved. We utilized a combination of conventional mutagenesis and the high precision methodology of unnatural amino acid incorporation to study extensively the gating interface of the mouse muscle nicotinic acetylcholine receptor. We found that charge reversal, charge neutralization, and charge introduction at the gating interface are often well tolerated. Furthermore, based on our data and a reexamination of previously reported data on γ -aminobutyric acid, type A, and glycine receptors, we concluded that the overall charging pattern of the gating interface, and not any specific pairwise electrostatic interactions, controls the gating process in the Cys loop superfamily.

The Cys loop superfamily of neurotransmitter-gated ion channels plays a prominent role in mediating fast synaptic transmission. Receptors for acetylcholine (nicotinic ACh receptor, nAChR),² serotonin (5-HT₃ receptor), γ -aminobutyric acid (GABA, types A and C receptors), and glycine are known, and the receptors are classified as excitatory (cation-conducting; nAChR and 5-HT₃) or inhibitory (anion-conducting; GABA and glycine). Malfunctions in these receptors are responsible for a number of “channelopathies,” and the receptors are targets of pharmaceutical efforts toward treatments for a wide range of neurological disorders, including Alzheimer disease, Parkinson disease, addiction, schizophrenia, and depression (1, 2). The receptors share a common architecture, are significantly homologous, and are known to have evolved from a single ancestral gene that coded for an ACh receptor.

The gating mechanism for the Cys loop superfamily is one of the most challenging questions in molecular neuroscience. At issue is how the

binding of a small molecule neurotransmitter can induce a structural change in a large, multisubunit, integral membrane protein sufficient to open (gate) a previously closed ion channel contained within the receptor (3, 4). All evidence indicates that the neurotransmitter-binding site is quite remote (50–60 Å) from the channel gate, the region that blocks the channel when the neurotransmitter is absent and that must move to open the channel.

The quest for a gating mechanism has been greatly aided by several recent structural advances. First, crystal structures of the soluble acetylcholine-binding protein (AChBP) (5–7), which is homologous to the extracellular domain of the nAChR and, by extension, other members of the superfamily, provide a good sense of the layout of the agonist-binding site and its relationship to the rest of the receptor. Second, continued refinement of cryo-EM images of the *Torpedo* nAChR by Unwin and co-workers (8–10), incorporating insights gained from the AChBP structure, has produced a full atomic scale model (Protein Data Bank code 2BG9) of the nAChR. It is important to appreciate from the outset that 2BG9, although heuristically quite valuable, is not a crystal structure of the nAChR. It is a model built from low resolution data and homology modeling. Nevertheless, it represents a substantial advance for the field, and all modern attempts to obtain molecular scale information on the structure and function of Cys loop receptors must consider this as a starting point.

The full 2BG9 model of the nAChR (10) immediately suggested ways in which the agonist-binding site could couple to the transmembrane region and thus initiate gating. As summarized in Fig. 1, loops 2, 7, and 9 from the AChBP structure are oriented toward the transmembrane region, and indeed, in 2BG9 these loops make contacts with parts of the transmembrane domain. Note that loop 7 is the eponymous Cys loop. The transmembrane region consists of four α -helices per subunit, labeled M1–M4. It is accepted that M2 lines all or most of the channel. Helix M1 extends out of the transmembrane region toward the extracellular domain, creating a segment termed pre-M1. Although M4 is somewhat separated from the rest of the protein in 2BG9, recent modeling studies produce a more compact structure in which M4 is more intimately involved (11). In particular, the C terminus of M4, a region we will term post-M4, can contact the extracellular domain. A key structure is the M2–M3 loop, a short connector between the two transmembrane helices. Topological considerations have long placed this loop at the interface between the transmembrane and extracellular domains. That expectation was resoundingly confirmed by Protein Data Bank code 2BG9, and many workers have anticipated that this loop could play an important role in gating. Indeed, recent work (12) has established that a key proline at the apex of the M2–M3 loop provides the conformational switch that gates the channel in the 5-HT₃ receptor.

Several groups have attempted to identify key interactions in the interface between the extracellular domain and the transmembrane domain, and we discuss some of these results below. This interface contains a number of charged residues, and most efforts have focused

* This work was supported by the National Institutes of Health Grants NS-34407 and NS-11756. The costs of publication of this article were defrayed in part by the payment of page charges. This article must therefore be hereby marked “advertisement” in accordance with 18 U.S.C. Section 1734 solely to indicate this fact.

[§] The on-line version of this article (available at <http://www.jbc.org>) contains Figs. i–v and Table 1.

¹ To whom correspondence should be addressed: Division of Chemistry and Chemical Engineering, California Institute of Technology, 164-30, Pasadena, CA 91125. Tel.: 626-395-6089; Fax: 626-564-9297; E-mail: dadougherty@caltech.edu.

² The abbreviations used are: nAChR, nicotinic acetylcholine receptor; 5-HT₃, serotonin; GABA_A, γ -aminobutyric acid, type A; ACh, acetylcholine; HA, hemagglutinin; SuCh, succinylcholine.

Gating Interface of Cys Loop Receptors

on these, attempting to find crucial electrostatic interactions that regulate gating. Specific hydrophobic interactions have also been proposed (9, 13). Several interacting pairs have been identified in various receptors (14, 15), and specific gating models based on critical electrostatic interactions have been proposed (16–19). We note from the start, however, the curious fact that *none* of the proposed interactions is conserved across the superfamily. We have been puzzled by the notion that in this closely related family of receptors, the mechanism of action of the essential function of the receptors seems to vary from system to system.

In the present work we argue that specific, pairwise electrostatic interactions at the interface between the transmembrane and extracellular domains are not critical to gating. Rather, we argue it is the global charging of this region and the network of interacting ionic residues that are critical to receptor function. We present an overall analysis of charged interfacial residues in the Cys loop superfamily, extensive mutagenesis studies of potential electrostatic interactions in the nAChR, and a reconsideration of previously published data on other receptors to support the model. From such an analysis, a more nearly unified, but less precise, image of the gating mechanism in the Cys loop superfamily emerges.

MATERIALS AND METHODS

Mutagenesis and mRNA Synthesis—The mRNA that codes for the muscle type nAChR subunits (α , β , γ , and δ) was obtained by linearization of the expression vector (pAMV) with NotI, followed by *in vitro* transcription using the mMessage mMachine kit purchased from Ambion (Austin, TX). The mutations in all subunits were made following the QuickChange mutagenesis protocol (Stratagene).

Electrophysiology and Data Analysis—mRNAs of α , β , γ , and δ subunits were mixed in the ratio of 2:1:1:1 and microinjected into stage VI oocytes of *Xenopus laevis*. Electrophysiology recordings were performed 24–48 h after injection in two-electrode voltage clamp mode using the OpusXpress 6000A (Molecular Devices Axon Instruments). The holding potential was -60 mV and agonist was applied for 15 s (20). Acetylcholine chloride and succinylcholine chloride dihydrate were purchased from Sigma. All drugs were diluted to the desired concentrations with calcium-free ND96 buffer. Dose-response data were obtained for at least eight concentrations of agonists and for a minimum of five oocytes. Mutants with I_{\max} equal to or greater than 100 nA were defined as functional. EC_{50} and Hill coefficients were calculated by fitting the dose-response relation to the Hill equation. All data are reported as mean \pm S.E.

If saturation was not reached at 1000 μ M concentrations of acetylcholine, the EC_{50} value could not be calculated. For two mutations, α V46A and α V46T, a second mutation was incorporated at the 9' position of the β subunit (β L251S). This mutation is known to reduce the wild type EC_{50} to 1.2 μ M (21). The EC_{50} of the double mutant was then determined as described. For scatter plots (supplemental Figs. i–iii) the EC_{50} value of the double mutant was multiplied by 41.7 (50/1.2) to get a corrected EC_{50} value. The corrected EC_{50} value was used for the linear regression analysis.

EC_{50} values for succinylcholine were measured in the same manner. Maximal currents elicited by acetylcholine $I_{\max(\text{acetylcholine})}$ and by succinylcholine $I_{\max(\text{succinylcholine})}$ were measured sequentially at saturating concentrations on the same cells. The ratio of $I_{\max(\text{succinylcholine})}/I_{\max(\text{acetylcholine})}$ was calculated for each cell and is reported as mean \pm S.E.

Unnatural Amino Acid Suppression—The preparation of the unnatural amino acid *O*-methylthreonine is described elsewhere (21). *O*-Methylserine was purchased from Sigma and was protected and activated as described (22). Unnatural amino acids were conjugated to the

dinucleotide dCA and ligated to the truncated 74-nucleotide tRNA. The aminoacyl tRNA was deprotected by photolysis immediately prior to co-injection with mRNA containing an *amber* (TAG) stop codon at the site of interest. Negative and positive controls were employed as reported previously (20).

Bungarotoxin Binding and Western Blotting—48–72 h after injection, oocytes were prewashed with calcium-free ND96 buffer with 1 mg/ml bovine serum albumin, then transferred to the same buffer with the addition of 10 nM 125 I- α -bungarotoxin (PerkinElmer Life Sciences), and incubated for 1 h at room temperature (23). Oocytes were then washed four times and counted individually in a gamma counter. Oocytes injected with 50 nl of water were used to determine background. Mutants with more than five times the background reading are regarded to have sufficient expression.

In order to detect γ subunit incorporation for several mutants, an HA tag (hemagglutinin epitope) was incorporated at the C terminus in the γ subunit (position γ 497). 24–48 h after injection, 10–20 oocytes were incubated in hypotonic solution (5 mM HEPES, 5 mM NaCl) for 10 min, and the vitelline/plasma membranes were then isolated by physical dissection and centrifugation (24). The pelleted membranes were resuspended in 5 μ l of 2 \times SDS loading buffer, and SDS-PAGE was performed in 10% Tris-Cl ReadyGels (Bio-Rad). The samples were subjected to Western blot analysis using the anti-hemagglutinin antibody and visualized using an ECL detection kit (Amersham Biosciences).

RESULTS

Electrostatics at the Gating Interface—For the purposes of discussion and analysis, we have defined a “gating interface” between the extracellular domain and the transmembrane domain. It is comprised of the following six segments: three from the extracellular domain (all or parts of loops 2, 7, and 9) and three from the transmembrane domain (pre-M1, M2–M3, and post-M4). The precise residues considered are given in TABLE ONE. Unless otherwise noted, we will use the residue numbering system accepted for the nAChR α 1 subunit. The selection criterion for the gating interface was geometric; only residues that could reasonably be considered to experience a meaningful electrostatic interaction with another component of the gating interface were included. Because of the low resolution of the nAChR structure and the further uncertainty introduced by extrapolating to other Cys loop receptors, precise distance constraints were not applied. Rather, as illustrated in Fig. 1, we chose a contiguous band of residues in the region where the extracellular and transmembrane domains meet. Some leeway must be given in selecting possible interactions, as residues that are not in direct contact in 2BG9 could become so on transit from the closed state to the open state or going from one receptor to another. We recognize there is some arbitrariness to this assignment, but our studies suggested that extending the definition further out from the interface did not significantly impact the analysis. We will refer to the extracellular component (from loops 2, 7, and 9) and the transmembrane component (from pre-M1, M2–M3, and post-M4) when discussing the gating interface.

To search for patterns of charged residues, we considered the sequences of 124 subunits from the Cys loop superfamily, 74 cationic and 50 anionic channel subunits (see the Supplemental Material). TABLE ONE shows 22 representative subunits, 11 cationic (excitatory) channels and 11 anionic (inhibitory) channels, and also serves to define the various segments. TABLE TWO summarizes the analysis of the full collection of the 124 subunits. Shown for each segment of the interface are the number of cationic residues (Lys and Arg), the number of anionic residues (Asp and Glu), the net charge (Z), and the number of charged residues (N).

TABLE ONE

Selected sequences in the gating interface, highlighting cationic (italic) and anionic (boldface) residues

The abbreviations used are as follows: Tor, nAChR from *Torpedo californica*; nACh, nicotinic ACh receptor; 5-HT_{3A}, 5-HT₃ receptor, type A. All sequences were from human receptors except Tor and nACh $\alpha 1$, $\beta 1$, γ , δ , which were from mouse muscle.

	Loop 2	Loop 7	L9	Pre-M1	M2–M3 linker	Post-M4
Tor α	DEVNQI	IIVTHFPFDQ	EW	MQIRP	STSSAVPLIGKY	FAGRLIELSQEG
Tor β	NEKIEE	IKVMYFPFDW	QW	IQRKP	ETSLSVPIIRY	FLDASHNVPPDN
Tor γ	NEKEEA	IAVTYFPFDW	EW	IQRKP	ETSLNVPLIGKY	FLTGHFNQVPEF
Tor δ	KETDET	INVLYFPFDW	EW	IRRRP	ETALAVPLIGKY	FVMGNFNHPPAK
nACh $\alpha 1$	DEVNQI	IIVTHFPFDE	EW	MQRLP	STSSAVPLIGKY	FAGRLIELHQQG
nACh $\beta 1$	NEKDEE	IQVTYFPFDW	QW	IRRRP	ETSLAVPIIKY	FLDATYHLPPPE
nACh γ	NEREEA	ISVTYFPFDW	EW	IQRKP	ETSQAVPLISKY	FLMAHYNQVDDL
nACh δ	KEVEET	ISVTYFPFDW	EW	IRRRP	ATSMAIPLVGKF	FLQGVYINQPPLO
nACh $\alpha 4$	DEKNQM	IDVTFPFDQ	EW	IRRLP	STSLVIPLIGEY	FLPP--WLAGMI
nACh $\alpha 7$	DEKNQV	IDVRWFPPDV	EW	MRRRT	ATSDSVPLIAQY	LMSAPNFVEAVS
5HT3A	DEKNQV	LDIYNFPFDV	EW	IRRRP	ATAIGTPLIGVY	VMLWSIWQYA--
GABA $\alpha 1$	SDHDEE	MHLEDFPMDA	QY	LKRKI	KVAYATAM-DWF	LNREBPQLKAPT
GABA $\alpha 2$	SDDDEE	MHLEDFPMDA	QY	LKRKI	KVAYATAM-DWF	LNREBPVLGVSP-
GABA $\alpha 3$	SDDDEE	MHLEDFPMDV	QY	LKRKI	KVAYATAM-DWF	VNRESAIKGMIR
GABA $\alpha 4$	SDVEEE	MRLVDFPMDG	QY	LRRKM	KVSYLTAM-DWF	LSKDTMEKSESL
GABA $\alpha 5$	SDTEEE	MQLDFPMDA	QY	LKRKI	KVAYATAM-DWF	LNREBPVKGAA
GABA $\alpha 6$	SDVEEE	MRLVDFPMDG	QY	LQKRM	KVSYATAM-DWF	LSKDTMEVSSSV
GABA $\beta 1$	SEVNMD	MDLRRYPLDE	QF	LKRNI	KIPY-VKAIIDY	VN-----
GABA $\beta 2$	SEVNMD	MDLRRYPLDE	QF	LKRNI	KIPY-VKAIIDY	VN-----
GABA $\beta 3$	SEVNMD	MDLRRYPLDE	QF	LKRNI	KIPY-VKAIIDY	VN-----
Gly- $\alpha 1$	AETTMD	MDLKNFPMDV	QF	LERQM	KVSY-VKAIIDW	KIVRREDVHNQ-
Gly- $\alpha 2$	TETTMD	MDLKNFPMDV	QF	LERQM	KVSY-VKAIIDW	KIIRHEDVHKK-
	44 49	130 139	175	207 211	266 277	426

Although there is some variation, the typical gating interface contains 47 residues: 18 in the extracellular component and 29 in the transmembrane component. On average, 11.1 or 24% of these residues are charged. This is not significantly different from expectation based on the overall frequencies of occurrence of Asp, Glu, Arg, and Lys in proteins (July, 2004, Swiss Protein Database). Most of the residues of the gating interface are or can be easily imagined to be water-exposed to some extent; therefore, this global result is not surprising. Of the ~11 charged residues found in the gating interface, only two are universally conserved, Asp-138 and Arg-209. So, although all Cys loop receptors have a large number of ionic residues in the gating interface, their locations and absolute charges are variable.

Although the two components of the gating interface do not have the same number of amino acids, the total number of charges is essentially the same (5.7 versus 5.5) for the two. There is, however, a dramatic difference in the net charge of the two components. The extracellular component has an overall negative charge, averaging -3.9 over the 124 subunits considered. The transmembrane component has an overall positive charge, averaging $+2.3$. Thus, there is a global electrostatic attraction in the interface, holding together the extracellular component and the transmembrane component. This interfacial electrostatic interaction is not created by simply putting anions in the extracellular component and cations in the transmembrane component; typically, there are one cationic and five anionic side chains in the extracellular component but four cationic and two anionic side chains in the transmembrane component. We propose that it is the balance among all these charges that controls receptor function. With all these charges packed into a fairly compact space, we felt it more reasonable to consider a network of electrostatic interactions, rather than emphasizing any particular charged pair, as discussed below.

There is variability in the charging pattern. Considering only GABA_A subunits, $\alpha 1$ shows $Z = -6$ in the extracellular component and $Z = +4$

in the transmembrane component. In contrast, the $\alpha 4$ subunit shows $Z = -4$ in the extracellular component and $Z = +2$ in the transmembrane component. Despite the smaller Z values, the $\alpha 4$ subunit actually has more ionic residues overall than $\alpha 1$ ($n = 16$ versus 14).

Looking more closely, it is clear that loop 2 carries the most negative charge per residue, followed by loop 7. The largest net positive charge is associated with pre-M1. The total number of charges (N) is slightly larger for the inhibitory channels (average of 11.8 versus 10.7). The "additional charge" is usually cationic, as the net charge is slightly more positive for the inhibitory channels (-1.1 versus -1.9).

We propose that Cys loop receptors can function as long as the essential features of the electrostatic network are intact. As shown below, mutations that alter the charge balance are often well tolerated, apparently because they can be absorbed by the larger collection of charges. In fact, full charge reversals (replacing a plus with a minus or vice versa) are often quite acceptable. It appears that the important thing is to have a number of charges in this region, rather than any specific interaction.

Studies of the Muscle-type nAChR α Subunit—We have evaluated a number of residues in the gating interface by both conventional mutagenesis and unnatural amino acid mutagenesis (25). Many mutations are meant to parallel studies in other receptors, but as noted above, conservation is not strong across the family. We studied the embryonic mouse muscle nAChR with a subunit composition of $(\alpha 1)_2\beta 1\gamma\delta$. This receptor shows extremely high homology with and is thus directly comparable with the *Torpedo* receptor modeled by 2BG9. A goal of this work was to conduct an extensive survey of the gating interface, complementing the statistical analysis presented above. As such, we report the results of two-electrode voltage clamp determinations of EC_{50} , rather than the more time-consuming patch clamp studies of single channel behaviors. Because EC_{50} is a measure of channel function, it reflects contributions from agonist binding and gating. However, the residues studied are not part of the agonist-binding site and so seem unlikely to

Gating Interface of Cys Loop Receptors

FIGURE 1. Views of the gating interface. Structure is the full model of an α subunit of the *Torpedo* nAChR developed by Unwin (10) (Protein Data Bank code 2BG9). Regions of the gating interface, as defined in text, are color-coded. **A**, ribbon diagram, also including pairwise interactions from various studies that have been proposed to contribute to the gating mechanism. Even though they are from different receptors and could be important in different states of the receptor, they are mapped onto the *Torpedo* structure to provide some sense of relative spatial relationships. Distances range from ~ 6 to ~ 20 Å. Interactions are as follows: 1, Asp-138 to Lys-276 of muscle α nAChR; 2, Asp-138 to Arg-429 of muscle α nAChR; 3, Asp-57 to Lys-279 of GABA $_A$ $\alpha 1$ subunit; 4, Asp-149 to Lys-279 of GABA $_A$ $\alpha 1$ subunit; 5, Lys-215 to Asp-146 of GABA $_A$ $\beta 2$ subunit; 6, Lys-215 to Asp-139 of GABA $_A$ $\beta 2$ subunit; and 7, Lys-215 to Asp-56 of GABA $_A$ $\beta 2$ subunit. Interactions 1, 2, 4, and 5 all involve the same highly conserved Asp residue in loop 7. See text for discussion of these interactions. **B**, same view as **A** but with gating interface residues in space filling. **C**, view in **B** rotated 180° around vertical axis.

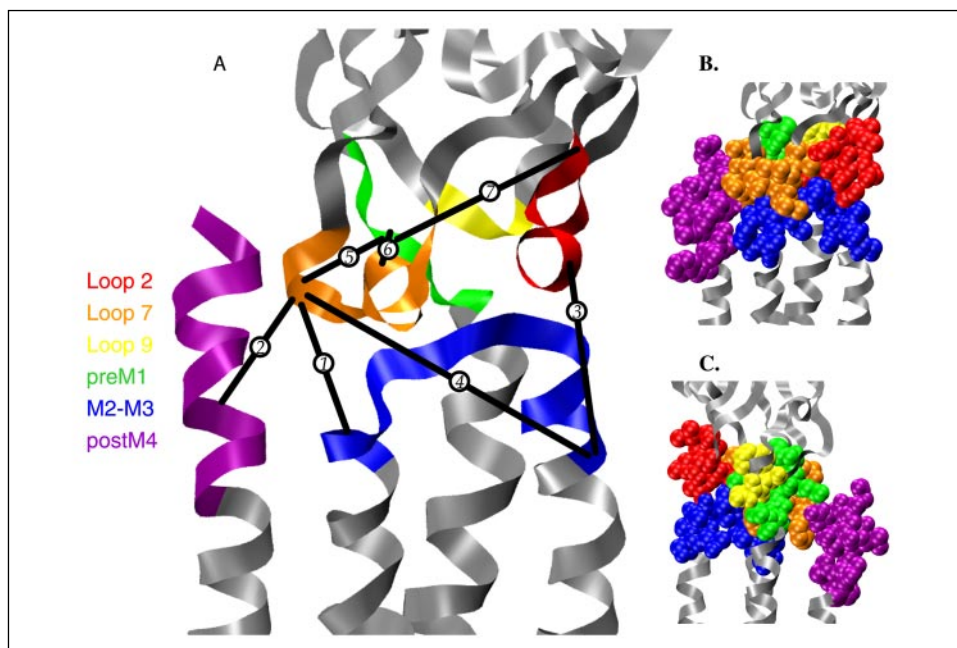


TABLE TWO

Charge characteristics of the gating interface

The abbreviations used are as follows: + indicates number of cationic residues (Lys and Arg); - indicates number of anionic residues (Asp and Glu); Z indicates overall charge; and N indicates the number of ionic residues.

	+	-	Z	N
Loop 2	0.5	2.3	-1.8	2.8
Loop 7	0.4	1.9	-1.5	2.4
Loop 9	0.0	0.5	-0.5	0.5
Pre-M1	2.3	0.1	2.2	2.3
M2-M3	1.0	0.8	0.2	1.8
Post-M4	0.6	0.7	-0.1	1.3
Extracellular	0.9	4.8	-3.9	5.7
Transmembrane	3.9	1.6	2.3	5.5
Gating interface	4.8	6.4	-1.6	11.1

contribute directly to binding. Furthermore, we show that representative mutations in the gating interface alter the relative efficacy of succinylcholine, a partial agonist of the mouse muscle nAChR (26), supporting a change in the gating of the mutants (14, 27). In addition, we recently showed that a range of mutations of a key proline at the heart of the gating interface in the M2-M3 loop of the 5HT $_3A$ receptor significantly affected EC $_{50}$ values but did not alter the binding properties of the receptor, establishing a role in gating (12). Extensive mutagenesis studies by Auerbach and co-workers (28) on loops 2 and 7 show that mutations of the sort considered here affect the gating equilibrium. As such, we concluded that the most reasonable interpretation of the changes in EC $_{50}$ values reported here is that they reflect alterations in channel gating behavior.

Our primary focus has been on the α subunits, as these make the largest contribution to the agonist-binding site and are thought to play a prominent role in the gating mechanism (29). In this section all mutations occurred in both copies of the mouse muscle α subunit; the results are given in TABLE THREE. In a subsequent section we will consider the non- α subunits.

The 2BG9 model features a particularly intimate interfacial interaction, that between Val-46 on loop 2 and a portion of the M2-M3 loop (9). A "pin-into-socket" arrangement was proposed, ascribing a critical

gating role to Val-46. Although it was immediately appreciated by many workers that Val-46 is not conserved in the Cys loop superfamily, the proposal merited investigation. Studies by Harrison and co-workers (13) on analogous residues in the GABA $_A$ $\alpha 1$ and $\beta 2$ subunits and the glycine receptor $\alpha 1$ subunit (the residue is His, Val, and Thr, respectively) provided no support for the pin-into-socket proposal.

We have explicitly evaluated Val-46 in the nAChR (TABLE THREE). We wished to determine whether a precise geometrical arrangement of the sort implied by a pin-into-socket interaction was essential for proper receptor function. Not surprisingly, the V46A mutation was substantially deleterious, whereas the more subtle V46I mutant showed near wild type behavior.

An advantage of the unnatural amino acid methodology is that it allows subtle stereochemical issues to be probed. If the side chain of Ile at position 46 points into a well defined pocket, one might anticipate that the isomeric *allo*-Ile, in which the side chain methyl and ethyl groups swap position relative to Ile, would show a significantly different interaction. In the event, the difference between Ile and *allo*-Ile is insignificant (TABLE THREE). The unnatural amino acid *O*-methylthreonine (OMe-Thr) is isosteric with Ile but inserts a more polar O in place of a CH $_2$ group (21). This subtle change is deleterious, raising the EC $_{50}$ >3-fold. The isomeric OMe-*allo*-Thr introduces a stereochemical swap that parallels the Ile/*allo*-Ile pair (Scheme 1). The difference between OMe-Thr and OMe-*allo*-Thr is ~ 5 -fold, corresponding to 1 kcal/mol at room temperature. This suggests that perhaps the side chain of position 46 is in a sterically well defined pocket, but one that can only be probed by polar oxygen atoms and not by hydrophobic groups such as CH $_2$.

Replacing Val-46 with much more polar groups like Thr (essentially isosteric to Val) and the anionic Asp and Glu seriously compromises receptor function. Radiolabeled α -bungarotoxin binding studies show that V46D and V46E channels are expressed in large enough quantities to detect macroscopic currents, but electrophysiology studies show only small (<300 nA) currents at 1 mM ACh, suggesting a shift to a much higher EC $_{50}$. Most surprisingly, however, the cationic residues Arg and Lys produce, in the first case, only a modest rise in EC $_{50}$ values, although the V46K mutant gives an EC $_{50}$ value ~ 50 -fold below wild type. The V46K mutation of the nAChR $\alpha 1$ subunit produces a loop 2 pattern

Gating Interface of Cys Loop Receptors

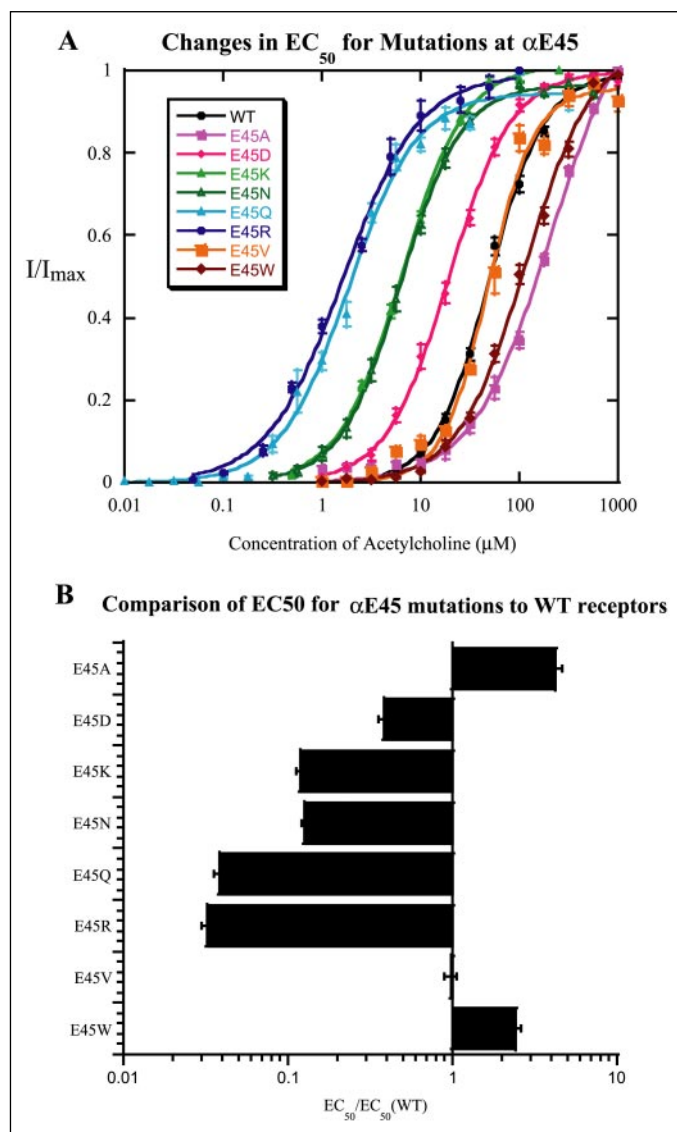


FIGURE 2. A variety of mutations at α Glu-45 are well tolerated. Charge neutralization (Asn and Gln) and charge reversal (Lys and Arg) both lower EC₅₀ values substantially, although mutations to hydrophobic residues (Ala, Trp, and Val) leave EC₅₀ values little changed. *A*, dose-response curves. *B*, ratios of mutant to wild type (WT) EC₅₀ values plotted for comparison.

Although the Asp-44 side chain points in the opposite direction to the Glu-45 side chain in 2BG9, the mutation pattern is similar. Both charge reversal and introducing a neutral but polar side chain lower EC₅₀ values.

Asn-47 in loop 2 of the nAChR α subunit aligns with Asp-57 of the GABA_A α 1 subunit, which, as discussed below, has been proposed to experience important electrostatic interactions (15). Auerbach and co-workers (28) have studied mutations at this site in the nAChR, including extensive single channel measurements. Auerbach and co-workers (28) found that N47K shows a decrease in EC₅₀ values, but N47D shows an increase. As noted above, the single channel studies of this and other loop 2 residues by Auerbach and co-workers (28) establish a role in setting the gating equilibrium for residues in this region.

Thus, at four consecutive residues in loop 2, Asp-44, Glu-45, Val-46, and Asn-47, introducing a positive charge lowers EC₅₀. At Asn-47 and Val-46 it has also been shown that introducing a negative charge has the opposite effect. These various side chains point in quite different directions in 2BG9. Although it is possible that all these side chains make

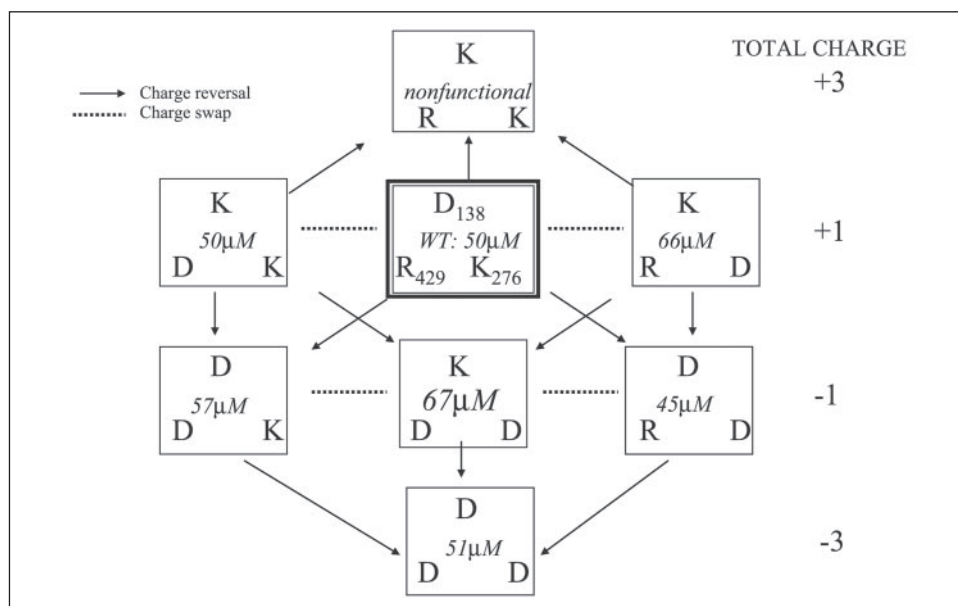
specific electrostatic contacts that are being modulated in similar ways by the mutations introduced, we conclude instead that it is the global negative charge of loop 2, not any specific pairwise interaction, that is essential to proper receptor function.

Asp-138 on loop 7 is completely conserved in the Cys loop superfamily. Others have investigated this site in other receptors (14, 15, 28). In the nAChR α subunit, charge reversal at this site incapacitates the receptor. Both D138K and D138R give nonfunctional receptors in that no response to ACh is seen, but labeling with the radioactive α -bungarotoxin shows that properly assembled receptors have reached the surface. Furthermore, milder disruptions of Asp-138 such as mutation to Asn, Ala, or Ser also give nonfunctional receptors. The charge conserving mutation D138E, however, gives near wild type behavior. All evidence shows that a negative charge at this site is essential to form a functional receptor.

A classic test for a specific ion pair interaction is the charge swapping experiment; *i.e.* if Asp-138 experiences an electrostatic interaction with a specific cationic residue, then the nonfunctional mutant often can be “rescued” by converting the cationic partner to an anion. In the nAChR, we considered two possible cationic partners to Asp-138: Lys-276 on M2–M3 and Arg-429 on post-M4 (pairwise interactions 1 and 2, respectively, in Fig. 1A). Both are fairly close to Asp-138 in 2BG9. Most interestingly, the nonfunctional D138K mutant can be returned to essentially wild type behavior by combination with *either* K276D or R429D (TABLE ONE and Fig. 3). This suggested that perhaps the 138/276/429 grouping should be considered as a charge triad, rather than a collection of pairwise interactions. As such, we evaluated all eight possible charge combinations for these three residues. The wild type is $-/+ / +$ (138/276/429); the nonfunctional D138K/D138R mutants are $+/+ / +$. The described double mutants that rescue the channel are $+/+ / -$ and $+ / - / +$. In fact, all seven combinations other than the $+/+ / +$ mutant give near wild type behavior (Fig. 3). It appears that the 138/276/429 grouping can compensate for a range of charge patterns, as long as $+/+ / +$ is avoided. It may seem surprising that the $- / - / -$ combination is viable. If these residues are physically close, we can anticipate that having three negative charges in proximity would alter the effective pK_a of one or more residues. This could lead to protonation of a carboxylate side chain and lessening of the electrostatic interaction. It is also possible that one or more water molecules mediate the interactions among 138/276/429. As will be discussed below, Asp-138 appears to be associated with a different charge triad in the GABA_A receptor.

Position 276 is conserved as a charged residue, either positive or negative, in the majority of ACh receptor subunits but not in other members of the superfamily. Position 429 is often but not always charged, being anionic in GABA receptors, cationic in glycine receptors, but neutral in nicotinic non- α subunits. Thus, the triad considered here is most likely specific to the nAChR α subunit. Residue 429 is on post-M4, and the M4 transmembrane helix is the furthest separated from the rest of the protein. In 2BG9, the C terminus of M4 is roughly 10 Å from the tip of loop 7. However, as mentioned above, computational studies move M4 closer to the rest of the protein and explicitly identify contacts between M4 and loop 7 (11). Also, it has been proposed from the computational work that during channel opening, M4 of the α 7 receptor moves closer to the other three transmembrane helices. In the linear free energy relation analysis by Auerbach and co-workers (34), the movement of an M4 precedes that of α M2. Based on the observations reported here, we conclude that in the open state of the nAChR, Arg-429 on post-M4 is one of the electrostatic interaction partners of Asp-138.

FIGURE 3. Charge reversal at α Asp-138 of the nAChR is rescued by charge swap at either of two sites: Arg-429 (post-M4) and Lys-276 (M2-M3). A charge triad is examined. Of the eight possible combinations, seven give near wild type (WT) behavior. Only the all-positive triad is deleterious.



We have also studied other positions of the M2–M3 linker. Four consecutive hydroxyl-containing residues, STSS, appear at positions 266 to 269 of the nAChR α 1 subunit. Various mutations at Ser-266 and Thr-267 do not shift EC₅₀ significantly (TABLE THREE). This includes mutations that would typically be considered fairly dramatic, in that a neutral residue is changed to an ionic residue. At Thr-267, conversion to a positive charge or a negative charge both result in halving EC₅₀.

Ser at position 269 has been probed previously by Auerbach and co-workers (35), who reported that an S269I mutation causes an EC₅₀ decrease of \sim 10-fold, mainly by increasing the channel opening rate constant. Based on this observation, it was proposed that position 269 moves from a polar to a nonpolar environment on channel opening, and so increasing hydrophobicity should favor the open state and lower EC₅₀. To probe this further, we incorporated the unnatural amino acid *O*-methylserine at position 269, an arguably more subtle way to reduce polarity than S269I. The mutant channel shows a 2-fold drop in EC₅₀, consistent with the expectation that an increase in hydrophobicity lowers EC₅₀, and the less perturbing Ser/OMeSer has a smaller effect.

Against this background, we were surprised to find that a change in the opposite direction (introducing either a positive or a negative charge at 269) also lowers EC₅₀; S269D and S269K show 4–5-fold drops, whereas S269E shows an astonishing 600-fold drop in EC₅₀. Certainly, Asp, Glu, and Lys are more polar than Ser, and so these results contradicted the just reached conclusion that hydrophobicity controls the behavior at position 269. We saw the same pattern for Ser-268; S268D, S268E, and S268K all show lower EC₅₀ values, with the Glu mutant again showing a very large drop. It is remarkable that at two consecutive sites in the M2–M3 loop, a region universally accepted to be involved in the gating transition, a serine can be converted to a cationic or an anionic residue, and the result is the same, the EC₅₀ drops.

Pre-M1 provides the covalent connection between the extracellular and transmembrane domains in the primary sequence, and there are 1–4 positive charges in this region throughout the ligand-gated ion channel family. One Arg (Arg-209 in the nAChR α 1 subunit) is completely conserved. Mutation to glutamine at the analogous arginine in the glycine receptor α 1 subunit causes hyperekplexia, an inherited channelopathy, and greatly diminishes receptor function (36). Among all the mutations at this site in the nAChR, only a charge-conserving mutation, R209K, gave a functional channel; charge reversal mutants

were nonfunctional. In 2BG9, the Arg-209 side chain projects between Glu-175 on loop 9 and Glu-45 on loop 2. Charge swapping experiments at this triad, however, show that the nonfunctional mutant R209E cannot be rescued by either E175R or E45R.

Loop 9 is located close to the transmembrane domain, between pre-M1 and loop 2. Chimera studies in Cys loop family members have characterized it as an indispensable contributor to proper channel coupling and functioning (37). In 2BG9 loop 9 has moved significantly closer to the transmembrane domain compared with the AChBP structure, suggesting that it is arranged differently when the transmembrane domain is present. Position 175 is located very close to the transmembrane domain and is counted as part of the charged interface. Glu-175 is conserved in the majority of excitatory channel subunits, although in inhibitory channels it is frequently replaced by a Gln. Mutation studies at this site show that a charge reversal increased the EC₅₀ but by a modest factor.

Studies of the Muscle-type nAChR Non- α Subunits—We have evaluated a large number of charged residues in the non- α subunits. Our primary emphasis has been on charge reversal and charge neutralization mutations (e.g. Glu \rightarrow Lys and Glu \rightarrow Gln). TABLE FOUR summarizes these data, showing for each site the consequences of charge reversal and charge neutralization. Again, to facilitate comparisons, we will use α 1 subunit numbering conventions in discussing these non- α subunits.

Typically, the changes seen in non- α subunits are not as dramatic as those seen in α , but some interesting observations can be made. In loop 2, which frequently has a larger number of charged residues (larger *N*) in the non- α subunits than in α , most of the charged residues are fairly tolerant of substitution, producing changes in EC₅₀ usually 2-fold or less, in contrast to the 10–30-fold changes often seen in α . At almost every site charge reversal is readily accommodated. Even at the very highly conserved Glu-45 site, charge reversal/neutralization is generally tolerated (TABLE FIVE). In fact, the triple mutant E45X in β , γ , and δ gave near wild type behavior for X = Gln, Arg, Lys, Asp, Asn, or Val. A 5-fold drop in EC₅₀ is seen for the triple A mutant, although a comparable E45A mutation of the two α subunits leads to a 4-fold rise in EC₅₀ values. Overall, the non- α loop 2 regions seem less sensitive to perturbation than α . As with the α subunit, efforts to correlate variations in EC₅₀ with various physicochemical properties of the side chains were unsuccessful.

TABLE FOUR
Mutations in the nAChR non- α subunits
 EC_{50} values are shown in μM .

	β						γ						δ						
	Mutation		Charge reversing		Charge neutralizing		Mutation		Charge reversing		Charge neutralizing		Mutation		Charge reversing		Charge neutralizing		
			EC_{50}	μ_H	EC_{50}	μ_H			EC_{50}	μ_H	EC_{50}	μ_H			EC_{50}	μ_H	EC_{50}	μ_H	
Loop 2	E45K/ E45Q		144 ± 7	1.5 ± 0.1	75 ± 4	1.3 ± 0.1	E45K/ E45Q		95 ± 2	1.4 ± 0.03	51 ± 1	1.4 ± 0.04	K44E/ K44Q		17 ± 1	1.1 ± 0.04	20 ± 1	1.3 ± 0.1	
	K46E/ K46Q		214 ± 28	1.1 ± 0.1	27 ± 3	1.3 ± 0.1	R46E/ R46Q		132 ± 5	1.3 ± 0.1	76 ± 8	1.1 ± 0.1	E45K/ E45Q		25 ± 1	1.5 ± 0.1	28 ± 2	1.2 ± 0.1	
	D47K/ D47N		28 ± 2	1.4 ± 0.1	56 ± 4	1.4 ± 0.1	E47K/ E47Q		29 ± 1	1.2 ± 0.04	21 ± 1	1.2 ± 0.1	E47K/ E47Q		11 ± 0.3	1.5 ± 0.1	22 ± 1	1.4 ± 0.1	
	E48K/ E48Q		69 ± 1	1.4 ± 0.03	22 ± 3	1.2 ± 0.2	E48K/ E48Q		135 ± 6	1.3 ± 0.1	31 ± 1	1.2 ± 0.03	E48K/ E48Q		44 ± 1	1.3 ± 0.1	30 ± 2	1.4 ± 0.1	
	E49K/ E49Q		26 ± 1	1.4 ± 0.04	21 ± 2	1.5 ± 0.1													
	D138K/ D138N		44 ± 7	1.5 ± 0.3	100 ± 3	1.4 ± 0.04	D138K/ D138N		35 ± 2	1.4 ± 0.1	34 ± 1	1.3 ± 0.1	D138K/ D138N		57 ± 9	1.2 ± 0.2	46 ± 3	1.5 ± 0.1	
PM1	R208E/ R208Q		25 ± 1	1.2 ± 0.04	26 ± 1	1.4 ± 0.1							R208E/ R208Q		16 ± 1	1.3 ± 0.1	23 ± 1	1.1 ± 0.1	
	R209E/ R209Q		93 ± 6	1.2 ± 0.1	37 ± 1	1.5 ± 0.1	R209E/ R209Q		27 ± 1	1.5 ± 0.1	75 ± 3	1.2 ± 0.04	R209E/ R209Q		20 ± 2	1.5 ± 0.1	33 ± 2	1.1 ± 0.1	
	K210E/ K210Q		27 ± 1	1.5 ± 0.1	55 ± 2	1.7 ± 0.1	K210E/ K210Q		4.9 ± 0.2	1.2 ± 0.1	8.2 ± 0.4	1.6 ± 0.1	K210E/ K210Q		3.9 ± 0.1	1.3 ± 0.03	5.3 ± 0.3	1.1 ± 0.1	
M2-M3 linker	D262K/ D262N		21 ± 2	1.1 ± 0.1	17 ± 1	1.6 ± 0.1	K262E/ K262Q		13 ± 0.2	1.5 ± 0.04	32 ± 1	1.4 ± 0.04	K262E/ K262Q		16 ± 0.4	1.3 ± 0.03	27 ± 1	1.3 ± 0.03	
	K263E/ K263Q		81 ± 4	1.3 ± 0.1	17 ± 1	1.6 ± 0.1	K263E/ K263Q		45 ± 1	1.3 ± 0.04	31 ± 1	1.3 ± 0.03	R263E/ R263Q		79 ± 2	1.3 ± 0.04	29 ± 5	1.2 ± 0.2	
	E266K/ E266Q		80 ± 1	1.3 ± 0.02	33 ± 2	1.2 ± 0.1	E266K/ E266Q		44 ± 4	1.3 ± 0.1	48 ± 7	1.0 ± 0.1							
	K276E/ K276Q		27 ± 1	1.4 ± 0.1	19 ± 1	1.5 ± 0.1	K276E/ K276Q		18 ± 2	1.3 ± 0.1	26 ± 1	1.5 ± 0.1	K276E/ K276Q		14 ± 1	1.3 ± 0.1	17 ± 1	1.5 ± 0.1	

TABLE FIVE

Mutations at Glu-45

EC₅₀ values are shown in μM.

Glu-45 mutant	α		β		γ		δ		β γ δ triple mutation	
	EC ₅₀	n _H	EC ₅₀	n _H	EC ₅₀	n _H	EC ₅₀	n _H	EC ₅₀	n _H
Gln	1.9 ± 0.1	1.3 ± 0.1	75 ± 4	1.3 ± 0.1	51 ± 1	1.4 ± 0.04	28 ± 2	1.2 ± 0.1	31 ± 2	1.2 ± 0.1
Arg	1.6 ± 0.1	1.0 ± 0.1	128 ± 4	1.4 ± 0.04	69 ± 2	1.3 ± 0.3	19 ± 1	1.4 ± 0.1	45 ± 4	1.4 ± 0.2
Lys	6.5 ± 0.3	1.4 ± 0.1	144 ± 7	1.5 ± 0.1	95 ± 2	1.4 ± 0.03	25 ± 1	1.5 ± 0.1	79 ± 8	1.1 ± 0.1
Asn	6.3 ± 0.1	1.4 ± 0.1	22 ± 1	1.1 ± 0.04	18 ± 1	1.3 ± 0.1	90 ± 4	1.0 ± 0.03	72 ± 3	1.2 ± 0.05
Asp	19.2 ± 0.5	1.4 ± 0.1	62 ± 4	1.1 ± 0.05	77 ± 4	1.2 ± 0.04	29 ± 2	1.1 ± 0.1	50 ± 3	1.2 ± 0.1
Val	49 ± 4	1.9 ± 0.2	88 ± 4	1.0 ± 0.04	37 ± 0.4	1.2 ± 0.02	34 ± 1	1.3 ± 0.05	38 ± 1	1.1 ± 0.03
Ala	210 ± 20	1.1 ± 0.1	32 ± 3	1.0 ± 0.1	26 ± 1	1.2 ± 0.04	11 ± 1	1.2 ± 0.1	11 ± 0.4	1.2 ± 0.1

Although αD138K gives nonfunctional receptors that can be rescued by compensating charge-reversal mutations, D138K in β or δ subunits gives functional receptors with no large change in EC₅₀ values (TABLE FOUR). The γD138K mutant gave very low currents in response to acetylcholine. Similarly, charge reversals in pre-M1 at Arg-208, Arg-209, or Lys-210 are generally well tolerated in non-α subunits. The Lys-210 to Glu or Gln mutations in γ or δ subunits produce some of the largest changes in EC₅₀, showing a 5–10-fold drop in EC₅₀ for charge reversal/neutralization.

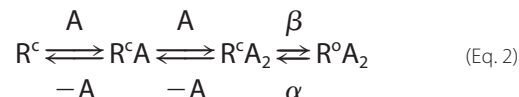
Finally, charge reversal/neutralization is well tolerated throughout the M2–M3 region in non-α subunits. Almost all changes lower EC₅₀ values, but the effects are all less than 3-fold. Apparent exceptions are the γE266K and γE266Q mutants, which gave little response to applied ACh. The previously employed test for surface expression, binding to α-bungarotoxin, was considered less reliable here, because receptors lacking the γ subunit can assemble on the cell surface and bind bungarotoxin. As such, we tested for expression by incorporating an HA epitope tag at the C terminus of the γ subunit and evaluating surface expression by using a Western blot. Previously, we have shown that the high sensitivity of anti-HA antibodies makes this a very sensitive probe of surface expression (38). For both the γE266K and γE266Q mutants, we find strong evidence for the γ subunit reaching the cell surface, indicating that these mutants do not disrupt folding, assembly, or transport of the receptor (data not shown). Most interestingly, γE266R and γE266N mutants do give significant currents, and the EC₅₀ values are only slightly higher than the wild type receptor.

It is clear that functionally, the non-α gating interfaces play a less important role than the α interfaces. Auerbach and co-workers (35) concluded that, in the M2–M3 loop, homology in sequence does not coincide with homology in function, and mutations in the δ subunit do not affect gating, consistent with our observations (34, 39, 40). From a structural perspective, however, the overall results from studies of non-α subunits highlight the remarkable tolerance of the gating interface. Dozens of charge reversal/neutralization perturbations are well tolerated, with the most common outcome being a small drop in EC₅₀. No evidence for highly specific, structurally or functionally important ion pair interactions is seen.

Studies of a Partial Agonist—To support our contention that mutations at the gating interface perturb the gating of the receptor rather than the agonist-binding site, we measured the relative efficacy (ε) of succinylcholine (SuCh), an nAChR partial agonist (26), for wild type receptor as well as for several representative mutants. The relative efficacy is defined as the ratio of the maximal current elicited by the partial agonist to the maximal current elicited by a full agonist (ACh) (Equation 1).

$$\epsilon = \frac{I_{\max,PA}}{I_{\max,FA}} = \frac{P_{\text{open},PA}}{P_{\text{open},FA}} \quad (\text{Eq. 1})$$

Equation 2 shows a highly simplified model of the agonist binding and receptor gating process.



$$P_{\text{open}} = \frac{\beta}{\alpha + \beta} \quad (\text{Eq. 3})$$

where R is receptor; c is closed; o is open; A is agonist; and β and α are the opening and closing rate constants, respectively. At saturating doses of agonist, all the receptors are forced into a diliganded state (RA₂), so differences in I_{max} for the two agonists are because of differences in P_{open}. As such, ε reflects the ratio of P_{open} values for the partial and full agonists (Equation 1). If a mutation has not altered the gating, but only the ligand binding of the receptor, the relative efficacies should be identical for the wild type and mutant receptors (14, 27).

For the wild type nAChR, P_{open} for ACh is very nearly 1 but P_{open} for succinylcholine is only 7.5% that for acetylcholine (ε = 0.075). As a control, we examined a previously studied mutant known to affect gating. Mutation of a universally conserved leucine at the 9' position of M2 to a more polar residue such as serine (βL251S) substantially reduces EC₅₀ values (21, 41, 42). This residue forms part of the hydrophobic gate of the channel and is quite remote from the agonist-binding site, establishing it as a gating residue. As shown in Fig. 4, the SuCh ε of the βL251S mutant is substantially increased over that of wild type. This indicates that P_{open} for SuCh has increased in the mutant, as expected for a mutation that substantially affects gating.

In the α subunit, the loop 2 mutations E45R and E45Q and the M2–M3 mutation S268E all decrease EC₅₀ more than 25-fold. All three mutations greatly increase ε, giving values near 1 (Fig. 4). This indicates that these mutations ease receptor opening, allowing SuCh to act as a full agonist. More importantly, the mutation E45V, which has no effect on EC₅₀, does not alter the ε of SuCh. The K210Q mutation in pre-M1 of the δ subunit shows only a small increase in ε. We evaluated this mutation both in the context of the otherwise wild type receptor and in receptors that contain the βL251S mutation, which moves the EC₅₀ values into a more manageable range. The small change in ε at this site supports the idea that the non-α subunits are less of a factor in channel gating.

Gating Interface of Cys Loop Receptors

Previous Work on the GABA_A and Glycine Receptors—Several important studies of possible electrostatic interactions in Cys loop receptors have appeared from Harrison and co-workers (14, 15) and Schofield and co-workers (18). In each case, a specific electrostatic interaction was identified by mutagenesis studies, emphasizing charge-reversal/charge-rescue strategies. Although we do not disagree with the fundamental observations of these efforts, we feel the results can be reinterpreted in the context of the charged interface model proposed here.

In the GABA_A receptor α 1 subunit, Harrison and co-workers (15) propose ion pair interactions between Lys-279 on the M2–M3 loop and two aspartates: Asp-57 on loop 2 and Asp-149 on loop 7 (pairwise interactions 3 and 4, respectively, in Fig. 1A). Here we used the GABA_A numbering. The analogous residues in the nAChR α subunit are as follows: Ser-266, Asn-47, and the previously discussed Asp-138; the proposed electrostatic interactions are not conserved. In the GABA_A receptor it is proposed that these “specific electrostatic interactions provide an intramolecular coupling mechanism” for the receptor. The

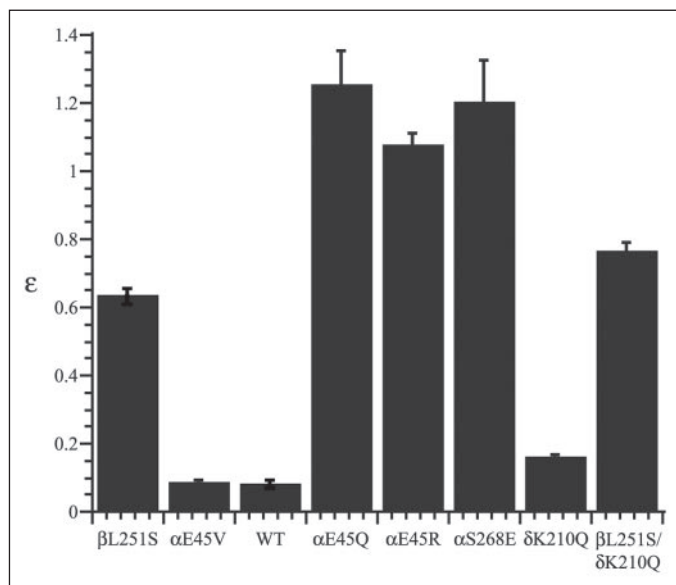


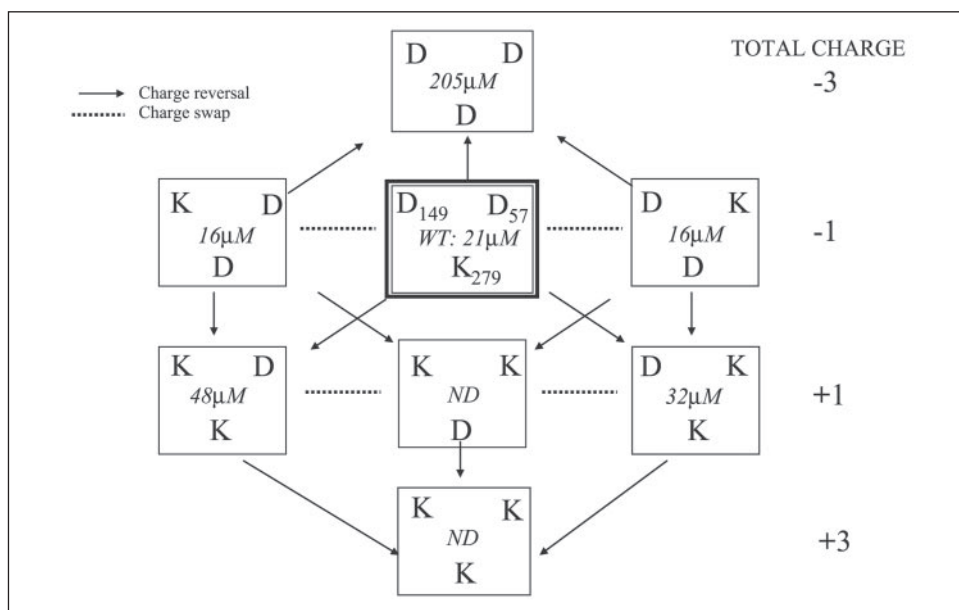
FIGURE 4. Relative efficacy (ϵ) of succinylcholine (versus ACh) for several variants of the nAChR. WT, wild type.

K279D mutation results in an ~ 10 -fold increase in EC_{50} values. However, full receptor function is regained when K279D is coupled with either D57K or D149K. In addition, it is proposed that Asp-149 and Lys-279 move closer to one another during the transition from closed to open state, presumably strengthening the ion pairing interaction.

In Fig. 5, we present these results in the same format as in our discussion of the charge triad of the nAChR given in Fig. 3. The mutation data, and the generally accepted notion that loop 2 and loop 7 straddle M2–M3, imply a triangular relationship between Asp-57, Asp-149, and Lys-279. Thus, the K279D mutation puts three negative charges in an array, which is apparently unfavorable. What is initially surprising, however, is that K279D is fully rescued by the single Asp/Lys mutations at either site 57 or site 149, producing receptors that actually function “better” (lower EC_{50}) than wild type. This means that although the D57K compensating mutation does rescue the 57 \cdots 279 interaction, 149 \cdots 279 is still a repulsive Asp \cdots Asp interaction, and yet the receptor shows EC_{50} values below wild type. The exact same situation holds with the single D149K mutation. Also, if 149 and 279 move closer to each other during gating, how could a structure in which they are both aspartates (D57K/K279D) gate more efficiently than wild type? If the key interactions were Asp-57 \cdots Lys-279 and Asp-149 \cdots Lys-279, the highly efficient gating of the D47K/K279D and D149K/K279D double mutants would be difficult to understand.

We propose that no specific ion pair interaction influences gating, but instead a cluster of charges similar to that described in Fig. 3 is important. The single K279D mutation puts three negative charges in a cluster and that is apparently unfavorable. In contrast, the wild type has a $-/-/+$ pattern (57/149/279), while the double mutants are $+/-/-$ and $-/+/-$. Any pattern of three charges adding up to -1 gives wild type behavior (or better). Other mutants were also evaluated (Fig. 5). Apart from $-/-/-$ (the original K279D mutant), the only severely deleterious cluster is $-/-/0$ (K279A), with a charge of -2 . Clusters with three charges that sum to $+1$ are not overly harmful. The $+/-/+$ mutant (D57K) shows only a 10% increase in EC_{50} , and $-/+/+$ (D149K) is much less than 2-fold higher. Surely these models are not of high enough precision to interpret such small differences. It seems the important thing is simply to have a cluster of charges that are not all the same, with specific ion pairing interactions being nonessential. Note the parallel behaviors of the 57/149/279 triad in the GABA_A α 1 subunit and

FIGURE 5. Analysis of previously published results for the GABA_A receptor α 1 subunit (15) in the same manner as in Fig. 3, suggesting a charge triad interaction. ND = not determined; WT, wild type.



the 138/276/429 triad in the nAChR $\alpha 1$ subunit (recall that nAChR 138 and GABA_A 149 are aligned residues). Great variation in the charging pattern is tolerated, with nonfunctional receptors resulting only from clusters with very high overall charge.

Evidence for a cluster can also be seen in the GABA_A $\beta 2$ subunit (14). The mutation K215D (pre-M1; aligns with nAChR $\alpha 1$ Gln-208) is deleterious; EC_{50} goes up 6.1-fold relative to wild type, corresponding to a penalty of 1.1 kcal/mol. This is substantially rescued by a compensating the D146K mutation (loop 7; aligns with nAChR $\alpha 1$ Asp-138; pairwise interaction 5 in Fig. 1A). EC_{50} is only 1.5-fold higher than wild type, corresponding to a 0.25 kcal/mol penalty. Thus, 77% $((1.1 - 0.25)/1.1)$ of the K215D penalty is rescued by D146K. However, other charge reversal mutations in the interfacial region also significantly rescue K215D. D139K (aligns with nAChR $\alpha 1$ Asp-131; pairwise interaction 6 in Fig. 1A) rescues 64%; D56K (loop 2; aligns with nAChR $\alpha 1$ Ile-49; pairwise interaction 7 in Fig. 1A) rescues 49%; E147K (aligns with nAChR $\alpha 1$ Gln-139) rescues 29%; and E52K (aligns with nAChR $\alpha 1$ Glu-45) rescues 25%. Stated differently, the range of EC_{50} values for the three best rescue mutants (D146K, D139K, and D56K) is substantially less than 2-fold. It seems risky to ascribe a special relationship to the 146–215 pair. Again, an image of Lys-215 as presenting a positive charge to a cluster of negative charges, such that it cannot itself be a negative charge, seems more sensible.

Studies of the glycine receptor from Schofield and co-workers (18) identified several charged residues on loops 2 and 7 that appeared to be important for gating. However, no particular pairwise relationships were uncovered, leading to the conclusion that these residues played a key role, but not through a “direct electrostatic” interaction.

DISCUSSION

We have defined for the Cys loop superfamily of receptors a gating interface that is composed of segments from the extracellular domain and the transmembrane domain that can reasonably be assumed to be juxtaposed, based on mutagenesis data and the best available structural information. Analysis of representative subunits from the superfamily indicates that there are a large number of ionic residues in the interface, but for the most part their precise locations and particular charges are not conserved. Many workers, including ourselves, have sought specific ion pair interactions that exert precise control over the gating process. However, we have come to believe that, with such a large number of charges clustered in a fairly compact region, it is not meaningful to isolate specific ion pairs. Rather, the global charging pattern of the gating interface is what controls gating. Receptors have evolved to create a compatible collection of charged residues that allows the receptor to assemble and also facilitates the existence of and interconversions among multiple states.

Although specific ionic residues are generally not conserved, overall charging patterns are. Within the gating interface the extracellular component carries a net negative charge, and the transmembrane component carries a net positive charge. This creates a global electrostatic attraction at the interface that maintains the integrity of the receptor as it transitions from the mostly β -sheet, relatively polar extracellular domain to the α -helical, nonpolar transmembrane domain.

Several lines of evidence support this way of thinking about the gating interface. We have studied a number of mutations that reverse, neutralize, or introduce charges. Typically, these are considered to be dramatic mutations, and they might be expected to be disruptive at a functionally important interface. However, one of the more remarkable features of the mutagenesis data of TABLES THREE to FIVE is the tolerance of the gating region to such charge disruptions. In fact, very often the EC_{50}

value is *lowered* by such strong perturbations. It seems hard to imagine that dramatic mutations involving the introduction or reversal of charge just happen to lead to a viable ion pair that is tolerated by the receptor. Rather, we believe the entire gating interface is tolerant of charge up to a point. A balancing act is in operation. By distributing a large number of charges across an interface, it is possible to have movement along that interface without creating adverse situations of like charges interacting strongly or a single charge in isolation in a poorly solvated environment. Consider Thr-267. Introducing charge is not deleterious at this site. In fact, converting the neutral Thr to a cation (T267K) or an anion (T267D) has the same effect, *i.e.* EC_{50} is halved. It appears that it is the number of charges that matters and not their particular identities. The same pattern is seen at Ser-268 and Ser-269. These residues are on the M2–M3 loop, a region that is universally accepted to be important in gating in the Cys loop superfamily of receptors (15, 35, 37, 43, 44). Loop 2 always carries a significant negative charge, and we show here that introducing a positive charge at any of four locations (Asp-44 to Asn-47) lowers the EC_{50} value. It thus appears that the negative charge stabilizes the closed state of the nicotinic receptor by interacting with a positive region. Based on Protein Data Bank code 2BG9 (8, 9), the M2–M3 loop seems the likely candidate for the positive region, but again the precise positioning of residues may be different.

A few charge reversals have been shown to be deleterious, and they can often be rescued by compensating charge reversals. The universally conserved Asp-138 is one such residue. In the nAChR $\alpha 1$, the GABA_A $\alpha 1$ (15) (where it is Asp-149) and GABA_A $\beta 2$ (14) (where it is Asp-146) compensating charge reversals can rescue the initial mutant (pairwise interactions 1, 2, 4, and 5 in Fig. 1A). However, the systems use completely different residues from apparently very different regions of the interface. There is certainly no universal pattern, and it appears that rather than conserving some specific pairwise interaction, it is the global charging pattern of the trio of residues that is most important. At another site, Asp-139 of GABA_A $\beta 2$ (14) (Ile-131 of nAChR $\alpha 1$), as many as five different sites can contribute to compensating a charge reversal, with a gradation of efficiencies.

We conclude that no one ion pair interaction is crucially important to gating across the entire Cys loop superfamily; clearly each receptor is different. However, it may be that there is a consistent mechanism across the superfamily, but one that does not single out any particular ion pair. Several groups have suggested that the extracellular domain and the transmembrane domain change relative positions going from the closed to the open state. Harrison and co-workers (15) propose that a residue on loop 7 moves closer to a residue on M2–M3 in the GABA_A receptor $\alpha 1$ subunit (Asp-149 and Lys-279, GABA_A numbering; pairwise interaction 4 in Fig. 1A). The detailed gating model from Unwin (10) emphasizes differential interactions between loops 2/7 (extracellular domain) and M2–M3 (transmembrane domain) along the gating pathway. We have proposed recently (12) that loop 2 and especially loop 7 interact with a specific proline on M2–M3 differentially in the open and closed states. In order to accommodate the structural rearrangement at the gating interface, the many charges involved must be comfortable in the environments provided by both the open and closed states and must also experience no highly adverse interactions in the transition state separating the two. With a large number of charges distributed throughout the interface, the extracellular domain and the transmembrane domain can slide past one another (or twist or turn or unclamp . . .) while maintaining an acceptable network of compensating charges throughout the process. During the movement, some ion pair interactions will strengthen and some will weaken, but crucial on/off interactions seem less critical. There are clearly many ways to

Gating Interface of Cys Loop Receptors

achieve the proper balance, and each system has evolved an ionic array that supports the desired gating behavior. The essential mechanism is universal across the Cys loop superfamily, but the precise details vary from system to system.

REFERENCES

1. Leite, J. F., Rodrigues-Pinguet, N., and Lester, H. A. (2003) *J. Clin. Investig.* **111**, 436–437
2. Paterson, D., and Nordberg, A. (2000) *Prog. Neurobiol.* **61**, 75–111
3. Changeux, J. P., and Edelman, S. J. (2001) *Curr. Opin. Neurobiol.* **11**, 369–377
4. Lester, H. A., Dibas, M. I., Dahan, D. S., Leite, J. F., and Dougherty, D. A. (2004) *Trends Neurosci.* **27**, 329–336
5. Brejc, K., van Dijk, W. J., Klaassen, R. V., Schuurmans, M., van Der Oost, J., Smit, A. B., and Sixma, T. K. (2001) *Nature* **411**, 269–276
6. Celie, P. H. N., Klaassen, R. V., van Rossum-Fikkert, S. E., van Elk, R., van Nierop, P., Smit, A. B., and Sixma, T. K. (2005) *J. Biol. Chem.* **280**, 26457–26466
7. Celie, P. H. N., Rossum-Fikkert, S. E. V., Dijk, W. J. V., Brejc, K., Smit, A. B., and Sixma, T. K. (2004) *Neuron* **41**, 907–914
8. Unwin, N., Miyazawa, A., Li, J., and Fujiyoshi, Y. (2002) *J. Mol. Biol.* **319**, 1165–1176
9. Miyazawa, A., Fujiyoshi, Y., and Unwin, N. (2003) *Nature* **423**, 949–955
10. Unwin, N. (2005) *J. Mol. Biol.* **346**, 967–989
11. Taly, A., Delarue, M., Grutter, T., Nilges, M., Le Novère, N., Corringer, P. J., and Changeux, J. P. (2005) *Biophys. J.* **88**, 3954–3965
12. Lummis, S. C. R. L., Beene, D. L., Lee, L. W., Lester, H. A., Broadhurst, R. W., and Dougherty, D. A. (2005) *Nature* **438**, 248–252
13. Kash, T. L., Kim, T., Trudell, J. R., and Harrison, N. L. (2004) *Neurosci. Lett.* **371**, 230–234
14. Kash, T. L., Dizon, M.-J. F., Trudell, J. R., and Harrison, N. L. (2004) *J. Biol. Chem.* **279**, 4887–4893
15. Kash, T. L., Jenkins, A., Kelley, J. C., Trudell, J. R., and Harrison, N. L. (2003) *Nature* **421**, 272–275
16. Schofield, C. M., Jenkins, A., and Harrison, N. L. (2003) *J. Biol. Chem.* **278**, 34079–34083
17. Kash, T. L., Trudell, J. R., and Harrison, N. L. (2004) *Biochem. Soc. Trans.* **32**, 540–546
18. Absalom, N. L., Lewis, T. M., Kaplan, W., Pierce, K. D., and Schofield, C. M. (2003) *J. Biol. Chem.* **278**, 50151–50157
19. Schofield, C. M., Trudell, J. R., and Harrison, N. L. (2004) *Biochemistry* **43**, 10058–10063
20. Cashin, A. L., Petersson, E. J., Lester, H. A., and Dougherty, D. A. (2005) *J. Am. Chem. Soc.* **127**, 350–356
21. Kearney, P. C., Zhang, H., Zhong, W., Dougherty, D. A., and Lester, H. A. (1996) *Neuron* **17**, 1221–1229
22. Kearney, P. C., Nowak, N. W., Zhong, W., Silverman, S. K., Lester, H. A., and Dougherty, D. A. (1996) *Mol. Pharmacol.* **50**, 1401–1412
23. Yoshii, K., Lei, Y., Mayne, K. M., Davidson, N., and Lester, H. A. (1987) *J. Gen. Physiol.* **90**, 553–573
24. Tong, Y., Brandt, G. S., Li, M., Shapovalov, G., Slimko, E., Karschin, A., Dougherty, D. A., and Lester, H. A. (2001) *J. Gen. Physiol.* **117**, 103–118
25. Nowak, M. W., Gallivan, J. P., Silverman, S. K., Labarca, C. G., Dougherty, D. A., and Lester, H. A. (1998) *Methods Enzymol.* **293**, 504–529
26. Placzek, A. N., Grassi, F., Papke, T., Meyer, E. M., and Papke, R. L. (2004) *Mol. Pharmacol.* **66**, 169–177
27. Colquhoun, D. (1998) *Br. J. Pharmacol.* **125**, 924–947
28. Chakrapani, S., Bailey, T. D., and Auerbach, A. (2004) *J. Gen. Physiol.* **123**, 341–356
29. Corringer, P. J., Le Novère, N., and Changeux, J. P. (2000) *Annu. Rev. Pharmacol. Toxicol.* **40**, 431–458
30. Karplus, P. A. (1997) *Protein Sci.* **6**, 1302–1307
31. Radzicka, A., and Wolfenden, R. (1988) *Biochemistry* **27**, 1664–1670
32. Chothia, C. (1975) *J. Mol. Biol.* **105**, 1–12
33. Zamyatnin, A. A. (1972) *Prog. Biophys. Mol. Biol.* **24**, 107–123
34. Mitra, A., Bailey, T. D., and Auerbach, A. (2004) *Structure (Camb.)* **12**, 1909–1918
35. Grosman, C., Salamone, F. N., Sine, S. M., and Auerbach, A. (2000) *J. Gen. Physiol.* **116**, 327–340
36. Castaldo, P., Stefanoni, P., Miceli, F., Coppola, G., Miraglia del Giudici, E., Bellini, G., Pascotto, A., Trudell, J. R., Harrison, N. L., Annunziato, L., and Tagliatela, M. (2004) *J. Biol. Chem.* **279**, 25598–25604
37. Bouzat, C., Gumilar, F., Spitamaul, G., Wang, H.-L., Rayes, D., Hansen, S. B., Taylor, P., and Sine, S. M. (2004) *Nature* **430**, 896–900
38. England, P. M., Zhang, Y., Dougherty, D. A., and Lester, H. A. (1999) *Cell* **96**, 89–98
39. Grosman, C., and Auerbach, A. (2000) *J. Gen. Physiol.* **115**, 637–651
40. Grosman, C., Zhou, M., and Auerbach, A. (2000) *Nature* **403**, 773–776
41. Filatov, G. N., and White, M. M. (1995) *Mol. Pharmacol.* **48**, 379–384
42. Labarca, C., Nowak, M. W., Zhang, H., Tang, L., Deshpande, P., and Lester, H. A. (1995) *Nature* **376**, 514–516
43. Campos-Caro, A., Sala, S., Ballesta, J. J., Vicente-Agullo, F., Criado, M., and Sala, F. (1996) *Proc. Natl. Acad. Sci. U. S. A.* **93**, 6118–6123
44. Lummis, S. C. R. (2004) *Biochem. Soc. Trans.* **32**, 535–539